RESEARCH PAPER

Leaf patch clamp pressure probe measurements on olive leaves in a nearly turgorless state

W. Ehrenberger[1,2], S. Rüger[2], C. M. Rodríguez-Domínguez[3], A. Díaz-Espejo[3], J.E. Fernández[3], J. Moreno[4], D. Zimmermann[1], V. L. Sukhorukov[1] & U. Zimmermann[2]

1 Lehrstuhl für Biotechnologie, Biozentrum, Universität Würzburg, Würzburg, Germany
2 ZIM Plant Technology GmbH, Hennigsdorf, Germany
3 Instituto de Recursos Naturales y Agrobiología (IRNAS-CSIC), Sevilla, Spain
4 Departamento de Biología Celular, Universidad de Sevilla, Sevilla, Spain

ABSTRACT

The non-invasive leaf patch clamp pressure (LPCP) probe measures the attenuated pressure of a leaf patch, P_p, in response to an externally applied magnetic force. P_p is inversely coupled with leaf turgor pressure, P_c, *i.e.* at high P_c values the P_p values are small and at low P_c values the P_p values are high. This relationship between P_c and P_p could also be verified for 2-m tall olive trees under laboratory conditions using the cell turgor pressure probe. When the laboratory plants were subjected to severe water stress (P_c dropped below *ca.* 50 kPa), P_p curves show reverse diurnal changes, *i.e.* during the light regime (high transpiration) a minimum P_p value, and during darkness a peak P_p value is recorded. This reversal of the P_p curves was completely reversible. Upon watering, the original diurnal P_p changes were re-established within 2–3 days. Olive trees in the field showed a similar turnover of the shape of the P_p curves upon drought, despite pronounced fluctuations in microclimate. The reversal of the P_p curves is most likely due to accumulation of air in the leaves. This assumption was supported with cross-sections through leaves subjected to prolonged drought. In contrast to well-watered leaves, microscopic inspection of leaves exhibiting inverse diurnal P_p curves revealed large air-filled areas in parenchyma tissue. Significantly larger amounts of air could also be extracted from water-stressed leaves than from well-watered leaves using the cell turgor pressure probe. Furthermore, theoretical analysis of the experimental P_p curves shows that the propagation of pressure through the nearly turgorless leaf must be exclusively dictated by air. Equations are derived that provide valuable information about the water status of olive leaves close to zero P_c.

INTRODUCTION

Irrigation is the largest consumer of water in (semi-) arid countries. At present it is very often more cost-efficient for a farmer to over-irrigate than to risk the crop being stressed either early or at a later stage. However, it is well known (see *e.g.* Möller *et al.* 2007; Netzer *et al.* 2009) that proper management of irrigation can result in enhanced productivity and/or quality. Furthermore, as pressure on available freshwater resources will increase dramatically in the future, farmers have to find ways of improving water use efficiency. Installation of sensors in the field, which measure the water demands of the crop or of fruit trees in real time over the entire vegetation period, provides a sustainable and therefore smart solution for reduction of water consumption. By using sensitive indicators, the effects of irrigation can be gauged, and thus optimised. Plant-based sensors that measure sap flow, diurnal changes in trunk diameter or leaf thickness, stem and leaf water potential, stomatal conductance, time domain reflectometry and/or canopy temperature have been suggested by several authors as feasible indicators for smart irrigation (Scholander *et al.* 1965; Boyer 1967; McBurney 1988; Cardon *et al.* 1994; Smith & Allen 1996; Burgess *et al.* 2000; Zweifel *et al.* 2000, 2001; Fernández *et al.* 2001, 2006; Goldhamer & Fereres 2001; Green *et al.* 2003; Nadler *et al.* 2003, 2006; Naor *et al.* 2008). Routine implementation of these techniques in crop fields, orchards and forests, however, failed for several practical and technical reasons (see Blank *et al.* 1995; Jones 2004).

There is convincing evidence that the non-invasive, Internet-based leaf patch clamp pressure (LPCP) probe recently introduced by Zimmermann *et al.* (2008) could meet the demands for precisely monitoring leaf water status of plants in real time. When clamped correctly, the probe measures relative changes in leaf turgor pressure, P_c. The measuring principle of the high-tech probe is quite simple. An external pressure, P_{clamp}, (generated by springs or – more elegantly – by magnets) is applied to a small patch of an intact leaf. The

pressure experienced by the cells is lower than P_{clamp} because of losses due to the compressibility and deformability of structural elements (such as the cuticle, cell walls and intercellular air spaces). The attenuation factor F_a for olive leaves is usually of the order of 0.2–0.3 and is assumed to be constant in the turgescent range of the leaf. Theory shows that the output pressure, P_p, sensed by the probe is dominated by the turgor pressure, P_c, of the cells. Both parameters are inversely coupled to each other. If the counter-acting turgor pressure is high (*e.g.* at pre-dawn), pressure transfer through the tissue is considerably attenuated; therefore, the output signal, P_p, is low. *Vice versa*, if the turgor pressure is low (*e.g.* at noon), a high P_p value is recorded. The prediction of the theoretically postulated power function relationship between P_p and P_c has been verified for many plant species, such as olive, grapefruit, grapevine, lianas, eucalypts, banana plants and oak trees, by concomitant P_p and leaf cell turgor pressure measurements using the minimal-invasive cell turgor pressure probe (Zimmermann *et al.* 2008, 2009; Westhoff *et al.* 2009; Rüger *et al.* 2010a,b). These measurements were performed in a range of P_c values between *ca.* 50 and 550 kPa.

Case studies on several crop and fruit trees have shown that the profile of the diurnal curves of the output signals of the probe change in a characteristic manner upon ongoing drought, reflecting the increasing difficulty to compensate turgor pressure losses by water uptake. Several parameters, such as the rise time of the P_p values in the morning (=P_c loss), the peak P_p values at noon (=maximum P_c loss), the decrease rate of the P_p values during the afternoon (=recovery phase of P_c) and/or the P_p values reached during the night (=maximum P_c) are affected by water stress and can be used as sensitive indicators for irrigation.

When P_c drops below *ca.* 50 kPa, the P_p peak values measured at noon increase dramatically, quite often exceeding the recommended measuring range of the probe (up to 250 kPa). This increase is expected in the light of the current theory and can be used (together with the other P_p parameters) as a clear-cut indication for severe water stress. Interestingly, olive trees (Ben-Gal *et al.* 2010; Fernández *et al.* 2011) under field conditions show a reversal of the diurnal P_p curves upon approaching the plasmolytic point, *i.e.* at noon minimum P_p values were recorded, whereas peak P_p values occurred during the night. The reversal of the P_p curves was completely reversible, even after a long period of drought. Upon watering, the diurnal P_p changes measured usually on leaves are re-established within a very short time. The reversal of the P_p curves cannot explicitly be explained by the current theory, suggesting that the P_p signal is exclusively affected by P_c changes (Zimmermann *et al.* 2008; Westhoff *et al.* 2009; Rüger *et al.* 2010a,b).

In this communication we show, theoretically, that the reversal of the P_p curves observed in olive trees can easily be explained by assuming that the attenuation factor, F_a, is no longer constant at P_c values close to zero due to an unfavourable ratio of air to water. Thus, at very low P_c values, F_a and not P_c is the dominant factor that affects the P_p signals. Fundamentals for the theoretical framework were diurnal P_p curves that were measured on small olive trees. These trees were subjected to several irrigation/non-irrigation regimes under constant laboratory conditions in order to exclude any effects of environmental factors on the P_p values.

MATERIAL AND METHODS

Plants

Probe measurements were performed under laboratory conditions on *ca.* 2-m tall olive trees (*Olea europaea*) planted in *ca.* 30-l pots filled with soil. The trees were subjected to a 9.5-h light/14.5-h dark regime. Ambient temperature and relative humidity were kept constant at 23°C and 55%, respectively. The light irradiation was *ca.* 196 µmol s^{-1} m^{-2} at the top and *ca.* 55 µmol s^{-1} m^{-1} at 1-m height.

Field experiments were made in 2010, in a hedgerow olive orchard with 4-year-old 'Arbequina' trees, close to Seville (37°15′N, 5°48′W). The tree rows were oriented north to south. Spacing between the rows was 4 m and between the trees 1.5 m (1667 trees ha^{-1}). The trees were, on average, 2.40-m tall and 2.12-m wide canopy. Some of the trees were subjected to a regulated deficit irrigation (RDI) treatment. The 60RDI treatments were scaled to a total irrigation amount of 60% of the crop evapotranspiration (ET$_c$) demand.

Leaf patch clamp pressure (LPCP) probe

The measuring principle of the non-invasive, online-monitoring LPCP probe (commercial name: ZIM-probe) is described in details elsewhere (Zimmermann *et al.* 2008, 2009; Westhoff *et al.* 2009). Briefly, a relatively small patch of a leaf is used as a sensing element for turgor pressure changes in the entire leaf. To this end, the stomata in the patch must be closed; simultaneously, the patch must be in hydraulic contact with its surroundings. This is achieved by positioning of an intact leaf between two planar circular metal pads integrated into two magnets. The lower pad contains a receptacle for integration of the pressure sensor chip. Leaf turgescence is determined by measuring the pressure transfer function of the leaf patch, *i.e.* by measuring the output leaf patch pressure, P_p, upon application of a constantly maintained external clamp pressure, P_{clamp} (up to 400 kPa). P_{clamp} can be varied by changing the distance between the upper and lower magnet.

Probes, together with the components for telemetric and mobile network-based data transfer to the Internet, were purchased from the company ZIM Plant Technology GmbH (Hennigsdorf, Germany). Real-time recording of the ZIM-probe data was provided by battery-powered telemetric transmitters, which were connected by cable to up to three probes. These transmitters sent wireless data together with the transmitter ID-code every 5 min *via* ISM (433 MHz) to a control station that logged and transferred the data with time stamps to a GPRS (*General Packet Radio Service*) modem linked to an Internet server, which provides the data in real time in chart and table form.

For proper function of the LPCP probe it is necessary that there is a homogeneous contact between the leaf patch and the pads of the two magnets. Only under these conditions can the pressure transfer function and thus turgor pressure be measured (see below). In the case of an inhomogeneous contact (*e.g.* point contacts), the probe is measuring changes in leaf thickness, which result in P_p changes that are opposite to those induced by changes in turgor pressure. Changes in leaf thickness of plants subjected to water stress are much smaller than turgor pressure induced changes.

Cell turgor pressure probe

The principle of the cell turgor pressure probe is described in detail elsewhere (Tyerman et al. 2004; Zimmermann et al. 2004; Bramley et al. 2007). The probe was inserted from the adaxial or abaxial side of the leaves into the parenchyma cells close to the midrib. The probe was inserted most likely into the spongy tissue because of the penetration depth of the microcapillary. Adaxial and abaxial measurements yielded similar results; therefore, the data were pooled. The cell turgor pressure probe was also used for the extraction of air from the leaves. To this end, the microcapillary filled with oil up to the very tip (under very small overpressure) was introduced perpendicular to the leaf surface. After release of tiny amounts of oil into the tissue, air – if present – could enter the tip.

Microscopy

Small fragments of leaf (2 mm^2) were fixed in 4% glutaraldehyde dissolved in 0.1 M cacodylate buffer, pH 7.2, for 3 h at 4°C and were post-fixed in 1% OsO_4 solution for 2 h at 4°C. Samples were dehydrated in a grade acetone series and embedded in Epon-812 (epoxy embedding medium; Sigma-Aldrich, St. Louis, MI, USA). Toluidine blue-stained semi-thin sections (0.5 μm) were viewed using a Leitz Aristoplan (Leica Mikroskopie and Systeme Gmbh, Wetzlar, Germany) light microscope.

Morphometric analysis

Forty cross-sections per group of treatments were investigated. The images were made with a digital camera (Leica DC-100, Leica Imaging Systems Ltd., Cambridge, England) and were analysed using a Leica Q-win program. Data were statistically evaluated with the Student-Newman-Keuls test. A statistically significant difference was considered when $P \leq 0.0001$. Average data are given as mean ± standard error.

RESULTS

Experimentals

Figure 1 shows part of a typical, long-term probe measurement on an olive tree subjected to several cycles of irrigation∕non-irrigation. About 4 days after stoppage of watering, the peak P_p values, which were reached at the end of the light phase (05:00 h), increased continuously over the following days, indicating continuous turgor pressure, P_c, loss. After some days, the increase in the peak P_p values was also accompanied by an increase of the P_p values during the dark phase. The original P_c values were obviously not restored during the dark phase, because of a water shortage. This was also reflected in an increase in the time needed for P_c recovery in the afternoon and at night (see enlargement in Fig. 2A and B). The turgor pressure recovery process starting in the afternoon could be approximated by an exponential function. The time constant, τ, of the exponential decreases of the P_p values increased from 54 min (just after watering) to 256 min, when the peak P_p value reached a maximum of ca. 95 kPa at the end of the light phase after 7 days (see the filled squares in Fig. 3). The increase of τ with ongoing non-irrigation could be fitted by an exponential function characterised by a time constant of 2.6 days.
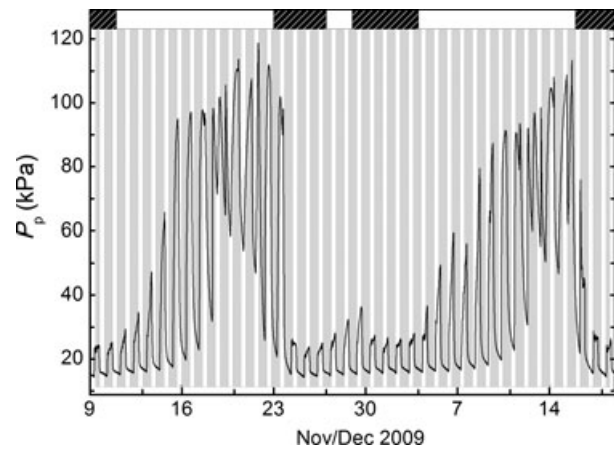

Fig. 1. Leaf patch clamp pressure probe measurements on a 2-m tall olive tree subjected to irrigation∕non-irrigation cycles under well-defined laboratory conditions. The figure shows part of a 2-month recording of the output patch pressure, P_p. Irrigation was stopped several times (marked by white areas above the panel). Note that ongoing non-irrigation resulted in a dramatic increase of the P_p value during the dark phase and of the peak P_p value during the light phase after 4 days. Note further reversal in the diurnal P_p profiles after 7 days of non-irrigation. At this time, P_p takes maximum values during the dark phase and minimum values during the light phase. Upon irrigation, the original P_p diurnal profiles are restored and measured again.

Cell turgor pressure probe measurements showed the well-known inverse relationship between P_p and P_c, taking into account the difficulties of P_c measurements on olive leaves. Inspection of the calibration curve in Fig. 4 reveals that a value of P_p = 95 kPa corresponded to a P_c value of ca. 50 kPa, providing evidence that the leaf cells were still turgescent. The turgor pressure range in which $P_p = f (1∕P_c)$ holds is denoted as state I (Fig. 2).

On day 7 after stoppage of watering, the P_p profile changed dramatically (Figs 1 and 2C). After switching on the light, the peak P_p value of 95 kPa was reached very rapidly compared to state I (3 h versus 11 h; Figs 1 and 2) and then decreased until at the end of the light phase a minimum value was reached. In the following dark hours the P_p values increased again. A peak value was reached at midnight, then again a decrease of the P_p values was observed until the light was switched on at 07:30 h. This diurnal curve shape of the P_p values was also recorded qualitatively on the following day. Measurements on the next day showed (Fig. 2D) that this state was intermediate (termed state II), because the diurnal P_p curves overturned into a stable state III measured also in the following days of non-irrigation. This state was characterised by a continuous increase of the P_p values during the dark phase (non-transpiration) and a continuous decrease of the P_p values during the light phase (transpiration). Both curves could be approximated by exponential functions. The time constant, τ, in dependency of the time after reaching state III, are given in Fig. 3 for the decrease of the P_p values during the light phase and for the increase of the P_p values during the dark phase (open circles and filled triangles, respectively). It is obvious from the figure that the τ values of the dark phase in state III reached values of up to
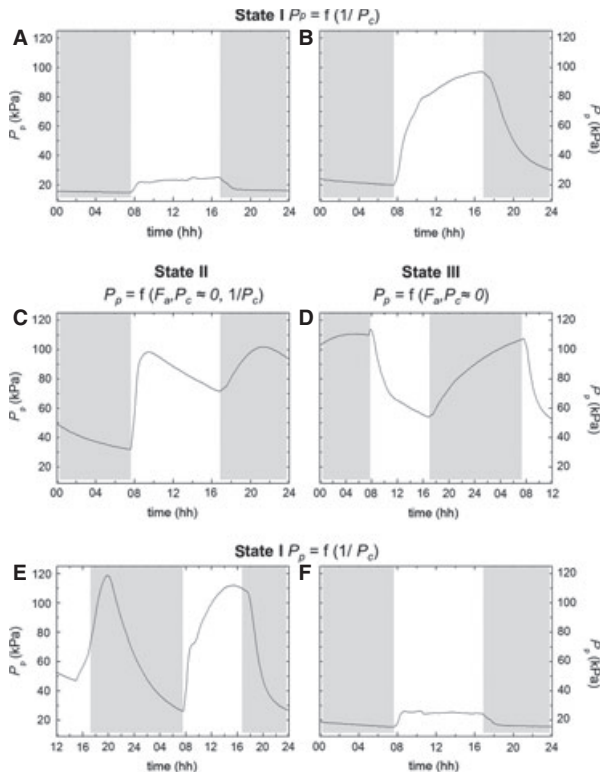
Fig. 2. Pressure transfer through the leaf patch under irrigation and non-irrigation conditions as predicted from equation (1). *State I* (turgescent state; upper graphs): P_p is inversely coupled to P_c ($P_p = f$ (1/P_c)); the attenuation factor $F_{a,const}$ related to turgor pressure-independent structural elements (such as cuticle, cell walls and air-filled spaces) is practically constant. Thus, the magnitude of P_p peaking at noon and the night P_p values depends exclusively on P_c (A: well-watered leaf; B: leaf subjected to 4-day drought). *State II* (very low turgor pressure values; C): F_a is no longer constant because of an unfavourable ratio of air to water in the leaf. Thus, P_p becomes a linear function of $F_{a,P_c\approx0}$, see equation (6), but still depends on P_c to some extent ($P_p = f$ ($F_{rma,P_c\approx0}$, 1/P_c)). *State III* (turgor pressure values close to zero): P_p depends exclusively on F_a ($P_p = f$ ($F_{a,P_c\approx0}$)) which assumes a minimum value during light phase (=large air spaces; maximum damping of pressure transfer) and a maximum value during dark phase (decrease of the air spaces by some water uptake and/or by a decrease in temperature: improvement of pressure transfer; D). Subsequent irrigation (arrow in E) resulted in an instant increase of the P_p values, followed by P_p decreasing during the dark phase and then by P_p peaking during the light phase (*state I*) on the following day (E). The amplitude of the P_p peaks decreased in the following 2 days, reaching the value measured under well-watered conditions (compare F with A).

Fig. 3. Effects of non-irrigation/irrigation cycles on the time constant τ of the exponential P_p decrease measured in *state I* after switch off of the light (filled squares), as well as the exponential P_p decrease after switch on of the light (open circles) and the exponential P_p increase after switch off of the light measured in *state III* (for approximation of the P_p curves in *state III* by exponentials, see Fig. 5). Non-irrigation periods are marked as white areas above the panel. Note that upon irrigation, the original τ values of *state I* were always re-established within a few days. Note further that the filled square (*state I*) and filled triangle (*state III*) data points could by fitted with an exponential function (solid line; time constant = 2.6 day). For further explanations, see Discussion.

and reached the original values of well-watered plants after 3 days (Fig. 3).

The phenomena described above were completely reversible, as shown by several irrigation/non-irrigation cycles, and were also found for different olive trees under field and laboratory conditions. It is also worthwhile to note that the reversal of the diurnal P_p curves upon severe drought could also be observed under field conditions; an example is given in Fig. 5. Whereas the leaves of the control trees remained in *state I* (Fig. 5A) over the summer period, trees that received only 60% of the total irrigation amount most of the time exhibited diurnal changes of P_p related to *state II* and *state III*, respectively (Fig. 5B).

Inspection of cross-sections of leaves subjected to severe drought, *i.e.* of leaves showing inverse diurnal P_p changes, had much larger areas of air spaces in the spongy mesophyll compared to well-watered leaves (0.5496 ± 0.012 μm^2 μm^{-2} *versus* 0.399 ± 0.008 μm^2 μm^{-2}; Fig. 6). This finding was supported by increased extraction of air from the leaves using the cell turgor pressure probe (a few microliters *versus* <1 µl in well-watered leaves).

Changes in leaf thickness as a possible reason for the reversal of the P_p curves in response to ongoing drought could be excluded. Leaf thickness measurements on well-watered leaves showed P_p curves that were opposite to those depicted in Figs 1 and 2. With ongoing drought, the P_p peaks decreased continuously towards their disappearance (data not shown).

Theoreticals

From a thermodynamic standpoint, the leaf patch can be considered as a black box consisting of turgescent cells and turgor-independent compressible structural elements, such as the cuticle, cell walls and air spaces. The output patch pressure P_p sensed by the sensor chip upon application of an external clamp pressure, P_{clamp}, is only determined by the leaf transfer function, T_f (V), where V is the leaf patch volume (Zimmermann *et al.* 2008; Westhoff *et al.* 2009):

600 min, whereas the τ values during the light phase were in the range measured for the τ values recorded during the turgor pressure recovery phase in *state I*. Subsequent irrigation (see arrow in Fig. 2E) resulted in an instant increase of the P_p values, followed by P_p decreasing during the dark phase and then peaking during the light phase on the following day. Peaking was nearly as high as observed the day before the overturning phenomena had started (compare Fig. 2E with 2B). After a further 2 days, the amplitude of the peak P_p values during the light phase was comparable to that measured on the well-irrigated plants (Fig. 2F *versus* 2A). Similarly, the τ values decreased accordingly after re-watering
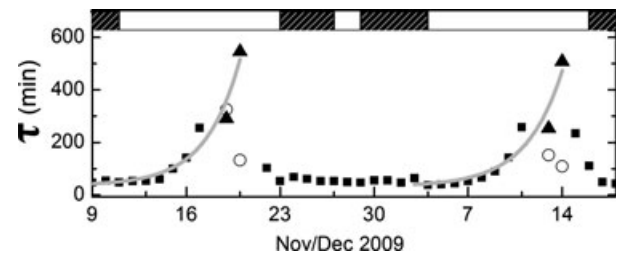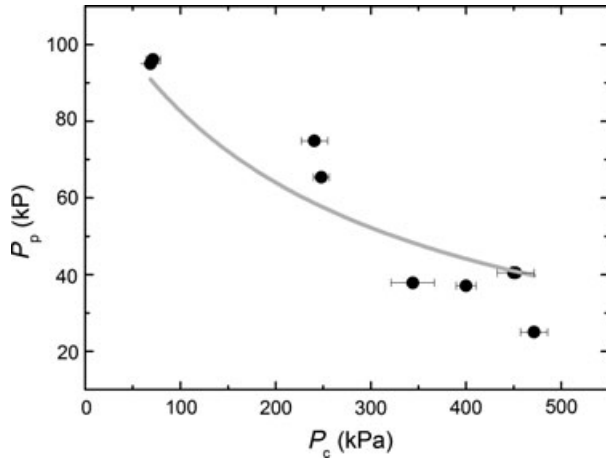
Fig. 4. Calibration of the leaf patch clamp pressure, P_p, measured in *state I* through short-term measurements of cell turgor pressure, P_c. Each P_c data point is an average turgor pressure value (±SD) taken from a 2- to 5-min measurement; the corresponding P_p values represent the mean (±SD) of at least three measuring points. Data were fitted using equation (5), with $F_{a,const} = 0.29$, $P_{clamp} = 398$ kPa, $a = 1.0$, $b = 244$ kPa, $R^2 = 0.87$. The dependency of P_p on P_c was found for more than 30 cells measured on different days.

$$P_p = T_f(V) \cdot F_{a,const} \cdot P_{clamp} \tag{1}$$

where $F_{a,const}$ is the leaf-specific attenuation factor that takes into account that only a fraction of P_{clamp} may arrive at the cell level due to P_c-independent pressure losses arising from the compressibility of the silicone used for the embedding of the sensor chip into the magnets and the leaf-specific structural elements.

T_f depends on the cellular volume of the leaf patch V, which, in turn, depends on P_c. The magnitude of volume changes upon changes in P_c is dictated by the average volumetric elastic modulus of the cells of the tissues, ε_P (Philip 1958):

$$\left(\frac{\partial P_c}{\partial V}\right)_T = \frac{\varepsilon_P}{V} \tag{2}$$

ε_P is a function of P_c and is given by equation (3) at constant temperature, T (Murphy & Ortega 1995):

$$\varepsilon_p = \varepsilon_0 - (\varepsilon_0 - \varepsilon_\infty) \cdot e^{-kP_c} \tag{3}$$

where k is a constant, ε_0 and ε_∞ are the volumetric elastic moduli at $P_c \approx 0$ and $P_c \approx \infty$, respectively. According to equation (3), ε_P reaches a plateau value for large P_c values. For smaller P_c values, *i.e.* $P_c < 1/k$, ε_P can be approximated by a linear dependency on P_c:

$$\varepsilon_p = aP_c + b \tag{4}$$

where $a = k \, (\varepsilon_\infty - \varepsilon_0)$ and $b = \varepsilon_0$. Both constants are equal or larger than unity. Combination of equation (1) with equation (2) and equation (4) yields:

$$P_p = \left(\frac{b}{aP_c + b}\right)^{\frac{1}{a}} \cdot F_{a,const} \cdot P_{clamp} \tag{5}$$

Eqation 5 demonstrates that P_p is a power function of P_c. This means that P_p increases more or less linearly with decreasing P_c over a large range of turgor pressures. However, at very low P_c (*ca.* <100 kPa) values, P_p increases over-proportional with a further decrease in P_c, provided that the attenuation factor can still be assumed to be constant. Equation (5) describes *state I* quite well, as shown by fitting of the data in Fig. 4 using appropriate values for the elastic constants a and b. For $P_c \approx 0$, equation (5) becomes equation (6):

$$P_p = F_{a,P_c \approx 0} \cdot P_{clamp} \tag{6}$$

In order to explain the experimental results, we have to assume that the attenuation factor in equation (6), $F_{a,P_c \approx 0}$, is no longer constant and becomes a function of time, t, around $P_c \approx 0$. The most likely reason for this is the diurnal variable accumulation of air in the leaf, as found experimentally (see Fig. 6). Thus, in the light of equation (6), we are driven to the conclusion that P_p becomes a linear function of this parameter because there is no physical reason to assume that P_{clamp} is changing upon approaching $P_c = 0$. *State II* (Fig. 2 C) obviously reflects the transient pressure range below *ca.* 50 kPa, where changes in $F_{a,P_c \approx 0}$ start to contribute to P_p, thus partly compensating for the inverse effect of P_c on P_p.

Inspection of the P_p curves of *state III* (Fig. 2D) shows that the increase of P_p during the dark regime and the decrease of P_p during the light regime can be approximated very well by assuming an exponential change of $F_{a,P_c \approx 0}$ with time. The mathematical analysis yields, for the increase of P_p during the dark regime:

$$F_{a,P_c \approx 0} = \left(F_{a,max} - F_{a,min}\right) \cdot \left(1 - e^{\frac{-t}{\tau_i}}\right) + F_{a,min} \tag{7}$$

and for the decrease of P_p during the light regime:

$$F_{a,P_c \approx 0} = \left(F_{a,max} - F_{a,min}\right) \cdot \left(e^{\frac{-t}{\tau_d}}\right) + F_{a,min} \tag{8}$$

where $F_{a,max}$ and $F_{a,min}$ correspond to the maximum and minimum P_p values, respectively, and τ_i and τ_d are the time constants of the corresponding exponential functions. In light of the experimental results, there are some good reasons to assume that $F_{a,max}$ is equal or very similar to $F_{a,const}$.

Figure 7A represents the theoretically expected change of $F_{a,P_c \approx 0}$ with time using equations (7) and (8), respectively, and Fig. 7B is the correlation between the P_p values and the corresponding $F_{a,P_c \approx 0}$ values of Fig. 7A. Inspection of Fig. 7B shows that a linear correlation exists between these two parameters, as expected in light of equation (6).

DISCUSSION

Direct turgor pressure measurements on olive leaves using the cell turgor pressure probe have verified (Fig. 4) that the patch pressure P_p measured with the LPCP probe is inversely coupled to P_c over a large P_c range, as predicted by equation (5). This was also found for other plant species (see literature quoted above). In the P_c range where equation (5) holds (termed *state I*; Figs 1 and 2), P_p peaking occurs during the
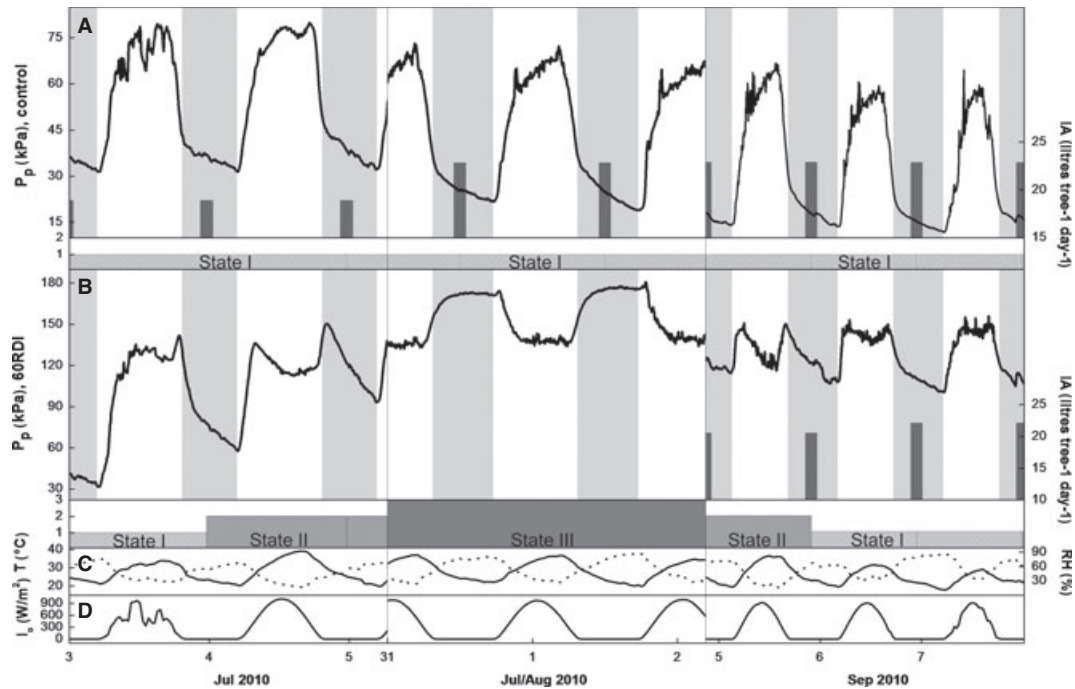
Fig. 5. Part of a long-term measurement of diurnal changes of P_p measured on east-oriented leaves of a control tree (A) and a 60RDI tree (B; RDI = regulated deficient irrigation) under field conditions. Irrigation amounts (IA) are denoted in grey bars; nocturnal hours are marked as grey columns. C: Ambient temperature (T; solid line) and relative humidity (RH; dotted line). D: 30-min averages of solar global radiation (I_o). Note that below the curves the state of turgescence of the leaves is given: State I = turgor pressures >*ca.* 50 kPa (P_p peaking at noon, minimum P_p values during the night), *state II* = turgor pressures <*ca.* 50 kPa (half inverse state: second peaking in late afternoon) and *state III* = very low turgor pressures (inverse state: minimum P_p values at noon and maximum values during the night). For further details, see text.

light phase (transpiration) and the minimum P_p values are recorded during the dark phase (non-transpiration).

We have demonstrated here for olive leaves that a reversal of the P_p curves occurred towards low turgor pressure values. The direct turgor pressure measurements have shown that the reversal of the diurnal P_p curves of olive leaves started below a turgor pressure, P_c, of about 50 kPa (*state III*). The transition from P_p peaking during the light phase (*state I*) to P_p peaking during the dark phase (*state III*) took place within

2–3 days (*state II*) under laboratory conditions. The reversal of the P_p curves was completely reversible after re-watering and was also found for olive trees under field conditions (Fig. 5).

Measurements of the pressure transfer function, and thus of P_c, require a uniform contact between the leaf patch and the pads of the magnetic probe. In the case of a non-uniform contact, mainly transpiration-induced changes in leaf thickness are recorded (Westhoff *et al.* 2009). Leaf thickness
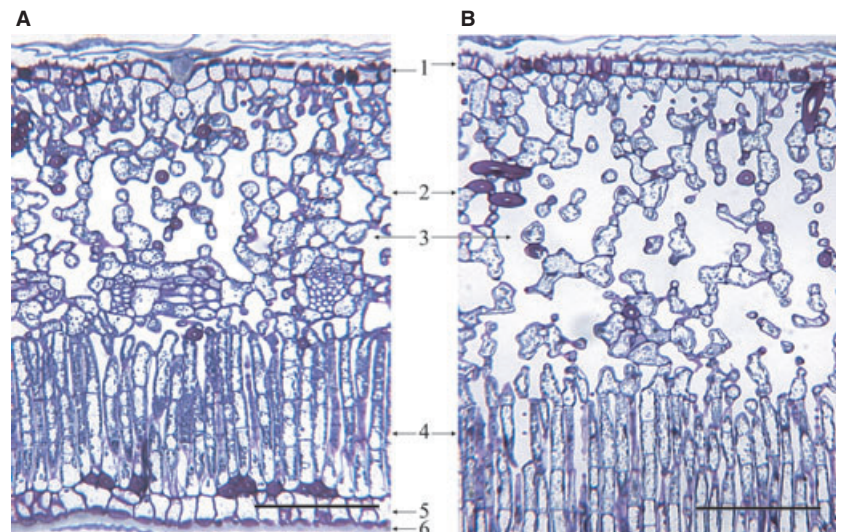

Fig. 6. Typical images of cross-sections of olive leaves under well-watered conditions (A; *state I*) and severe water stress (B; *state III*); bar = 100 μm. (1) Lower epidermis, (2) spongy mesophyll, (3) air space, (4) palisade mesophyll, (5) upper epidermis, (6) cuticle.
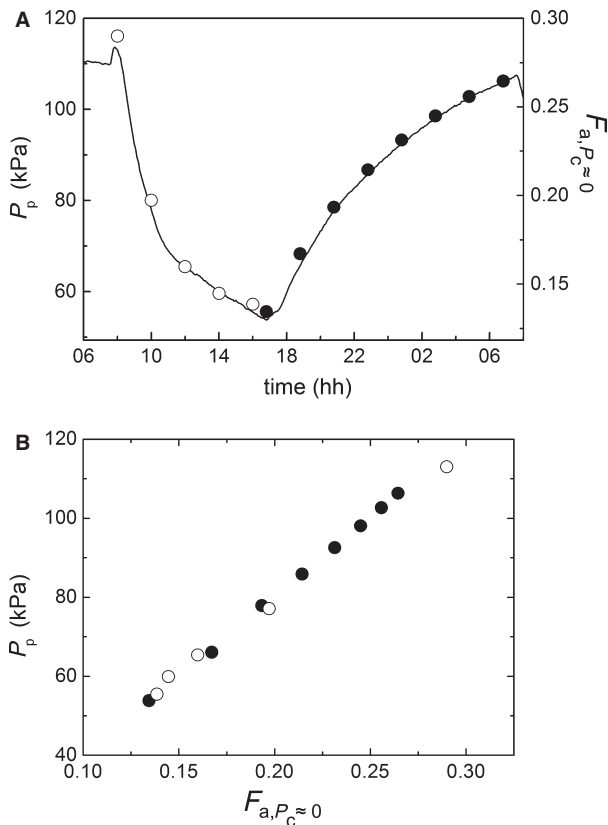
Fig. 7. Calculations of $F_{a,P_c \approx 0}$ from P_p changes measured in *state III*. A: Decrease of $F_{a,P_c \approx 0}$ as a function of time between 07:00 h (beginning of the light phase) and 04:00 h [open circles; light phase; equation (8)] and increase of $F_{a,P_c \approx 0}$ as a function of time between 04:30 h and 06:00 h of the following day [filled circles; dark phase; equation (7)]. B: Plots of the $F_{a,P_c \approx 0}$ values *versus* the corresponding P_p values for the light and dark phases.

assumes minimum values at high transpiration and *vice versa* maximum values at non-transpiration. Therefore, one possible explanation for the low-turgor pressure reversal of the P_p curves is that the probe is measuring changes in leaf thickness upon approaching $P_c \approx 0$ rather than the pressure transfer function of the leaf (equation 1). However, this explanation is very unlikely. Changes in leaf thickness are only expected in response to dramatic turgor pressure changes, *e.g.* when P_c drops from *ca.* 500 kPa (well-watered conditions; Fig. 4) down to 50–100 kPa (water-stressed conditions; Fig. 4). P_c changes in a range between 50 kPa and a few kPa may be too small to affect leaf thickness (see also Burquez 1987). Consistent with this, non-uniform clamping of the LPCP probe revealed (data not shown) that the changes in leaf thickness decreased and disappeared towards low turgor pressures. This was also found for other plants (Amos Naor, personal communication) and is a reason why leaf thickness measurements have not found wide applications in the last two decades.

There were also no visual indications for changes in the uniform contact between the leaf and the probe upon approaching $P_c \approx 0$ that could explain the reversal of the P_p curves as outlined above. Evidence for a uniform contact

even close to $P_c \approx 0$ also derived from the finding that after re-watering, P_p peaking during the light phase was re-established within 1 day (*state I*) without passing the transient *state II*. The amplitude of the P_p peaking during the light phase of the first day after watering was as high as the amplitude of P_p peaking measured just before the P_p reversal (compare Fig. 2E with 2B), indicating that there was a smooth transition from *state III* to *state I*. In the case of changes in the contact between the probe and the leaf patch, discontinuities after re-watering would be expected. Moreover, in the following 2 days the P_p amplitude decreased to the original value of well-watered trees. The decrease was quite similar to that observed when re-watering started before the P_p reversal occurred. The above findings and observations are obviously only consistent with the assumption of a constantly uniform contact between the probe and the leaf over the entire turgor pressure range from 0 kPa up to the maximum P_c values of 500 kPa.

Analysis of changes in the time constants, τ, with ongoing non-irrigation depicted in Fig. 3 suggests that the reversal of the P_p curves is related to dramatic changes in leaf water status around $P_c \approx 0$. In *state I*, τ is the time constant of the exponential decrease of P_p after the light is switched off. This phase reflects the process of turgor pressure regeneration (*e.g.* Zimmermann *et al.* 2009). As shown in Fig. 3, τ remains constant for about 3 days after stopping irrigation in order to increase then significantly with ongoing non-irrigation. The increase of τ can be described by an exponential function with a time constant of 2.6 days. Extrapolation of the exponential curve of *state I* to *state III* shows (see Fig. 3) that the τ values of the P_p increase recorded during the dark phase (but not the τ values of the P_p decrease recorded during the light phase) can be fitted by the same function. This suggests that the P_p increase phase reflects the phase of some turgor pressure regeneration close to $P_c \approx 0$. The build up of turgor pressure is obviously superimposed by a second, dominating process in the opposite direction.

This process is most likely initiated by the air in the leaves. Due to its high compressibility, air attenuates the pressure transfer through the leaf. Transpiring leaves will generally contain larger air spaces than non-transpiring ones (due to water uptake, and under field conditions due to lower temperatures during the night). Thus, attenuation of the external magnetic pressure will, in principle, be larger in transpiring plants than in non-transpiring ones. When the water supply of the leaves is sufficient and, in turn, the turgor pressure is quite high, the diurnal changes in the air amount in the leaves will be negligible. Thus, it is justified (and was verified experimentally) to assume that the attenuation factor, F_a, which takes – among other things – mainly pressure losses by compression of air spaces into account, is constant for a first and good approximation. However, the total amount of air within the leaf tissue is apparently increased dramatically with decreasing P_c below *ca.* 50 kPa. Support for this assumption was obtained from analysis of cross-sections through well-watered leaves and leaves subjected to severe drought. As shown in Fig. 6, the volume occupied by air increased considerably in leaves exhibiting inverse P_p curves (*state III*) compared to turgescent leaves (*state I*). Increased amounts of air were also found through extraction of air by using the cell turgor pressure probe.

As already mentioned above in the theoretical section, these findings and observations lead to the conclusion that the attenuation factor, F_a, can no longer be assumed to be constant at low P_c values. Since the contribution of P_c to the P_p signals is practically negligible [see the denominator of equation (5) and set $P_c = 0$], P_p becomes exclusively a linear function of $F_{a,P_c \approx 0}$ when *state III* is reached [see equation (6) and Fig. 7B]. Theory and the experiments show consistently (equations (7), (8) and Fig. 7A) that $F_{a,P_c \approx 0}$ changes exponentially with time. $F_{a,P_c \approx 0}$ reaches a maximum value (=minimum air-related losses of the external magnetic pressure) during the dark phase and a minimum value (=maximum air-related losses of the external magnetic pressure) during the light phase. The maximum $F_{a,P_c \approx 0}$ value of 0.26 reached at the end of the dark phase corresponds quite well with the F_a value determined for $P_c > ca.$ 50 kPa, supporting the view that during the dark phase some turgor pressure is built up by water uptake through the roots or by water movement within the plants.

Taken together, the above considerations demonstrate that the turgor pressure information that can be deduced from LPCP probe measurements is not restricted to the normal turgor pressure range. Rather, the theory shows that valuable information about the water supply to the leaves can also be extracted from measurements at extremely low turgor pressures. The surprising finding that the P_p reversal phenomenon was completely reversible after re-watering suggests that the air spaces play an important role in the water supply of olive leaves under severe water stress. It is well-known (see the review article of Zimmermann *et al.* 2004) that air spaces can create interfacial water flow (termed Marangoni streaming) through which water can still be shifted effectively to the leaf cells, even if the xylem is interrupted by gas bubbles due to cavitation. Future experiments must elucidate the proposed role of air spaces in more detail. Nevertheless, for agricultural water management, it is sufficient to point out that the P_p reversal phenomenon can be used as a powerful indicator for determination of the water stress state of olive trees.

ACKNOWLEDGEMENTS

REFERENCES

Ben-Gal A., Kool D., Agam N., van Halsema G.E., Yermiyahu U., Yafe A., Presnov E., Erel R., Majdop A., Zipori I., Segal E., Rüger S., Zimmermann U., Cohen Y., Alchanatis V., Dag A. (2010) Whole-tree water balance and indicators for short-term drought stress in non-bearing 'Barnea' olives. *Agricultural Water Management*, **98**, 124–133.

Blank K., Lamersdorf N., Dohrenbusch A., Murach D. (1995) Response of a Norway spruce forest ecosystem to drought/rewetting experiments at Solling, Germany. *Water, Air and Soil Pollution*, **85**, 1251–1256.

Boyer J.S. (1967) Leaf water potentials measured with a pressure chamber. *Plant Physiology*, **42**, 133–137.

Bramley H., Turner N.C., Turner D.W., Tyerman S.D. (2007) Comparison between gradient-dependent hydraulic conductivities of roots using the root pressure probe: the role of pressure propagations and implications for the relative roles of parallel radial pathways. *Plant, Cell and Environment*, **30**, 861–874.

Burgess S.S.O., Adams M.A., Bleby T.M. (2000) Measurement of sap flow in roots of woody plants: a commentary. *Tree Physiology*, **20**, 909–913.

Burquez A. (1987) Leaf thickness and water deficits in plants: a tool for field studies. *Journal of Experimental Botany*, **38**, 109–114.

Cardon Z.G., Mott K.A., Berry J.A. (1994) Dynamics of patchy stomatal movements, and their contribution to steady-state and oscillating stomatal conductance calculated using gas-exchange techniques. *Plant, Cell and Environment*, **17**, 995–1007.

Fernández J.E., Palomo M.J., Díaz-Espejo A., Clothier B.E., Green S.R., Gíron I.F., Moreno F. (2001) Heat-pulse measurements of sap flow in olives for automating irrigation: tests, root flow and diagnostics of water stress. *Agricultural Water Management*, **51**, 99–123.

Fernández J.E., Durán P.J., Palomo M.J., Díaz-Espejo A., Charmorro V., Gíron I.F. (2006) Calibration of sap flow measurements by the compensation heat-pulse method in olive, plum and orange trees: relations with xylem anatomy. *Tree Physiology*, **26**, 719–728.

Fernández J.E., Rodríguez-Domínguez C.M., Perez-Martin A., Zimmermann U., Rüger S., Martín-Palomo M.J., Torres-Ruiz J.M., Cuevas M.V., Sann C., Ehrenberger W., Diaz-Espejo A. (2011) Online monitoring of tree water stress in a hedgerow olive orchard using the leaf patch clamp pressure probe. *Agricultural Water Management*, **100**, 25–35.

Goldhamer D., Fereres E. (2001) Irrigation scheduling protocols using continuously recorded trunk diameter measurements. *Irrigation Science*, **20**, 115–125.

Green S., Clothier B., Jardine B. (2003) Theory and practical application of heat pulse to measure sap flow. *Agronomy Journal*, **95**, 1371–1379.

Jones H.G. (2004) Irrigation scheduling: advantages and pitfalls of plant-based methods. *Journal of Experimental Botany*, **407**, 2427–2436.

McBurney T. (1988) A temperature-controlled plant psychrometer. *Plant and Soil*, **109**, 271–275.

Möller M., Alchanatis V., Cohen Y., Meron M., Tsipris J., Ostrovsky V., Sprintsin M., Cohen S. (2007) Use of thermal and visible imagery for estimating crop water status of irrigated grapevine. *Journal of Experimental Botany*, **58**, 827–838.

Murphy R., Ortega J.K.E. (1995) A new pressure probe method to determine the average volumetric elastic modulus of cells in plant tissues. *Plant Physiology*, **107**, 995–1005.

Nadler A., Raveh E., Yermiyahu U., Green S.R. (2003) Evaluation of TDR use to monitor water content in stems of lemon trees and soils and their responses to water stress. *Soil Science Society of America Journal*, **67**, 437–448.

Nadler A., Raveh E., Yermiyahu U., Green S.R. (2006) Stress-induced water content variations in mango stem by time domain reflectometry. *Soil Science Society of America Journal*, **70**, 510–520.

Naor A., Naschitz S., Peres M., Gal Y. (2008) Responses of apple fruit size to tree water status and crop load. *Tree Physiology*, **28**, 1255–1261.

Netzer Y., Yao C., Shenker M., Bravdo B., Schwartz A. (2009) The use of crop coefficients for skilled irrigation of table grapes trained to a large trellis system. *Irrigation Science*, **27**, 109–120.

Philip J.R. (1958) The osmotic cell wall, solute diffusibility, and the plant water economy. *Plant Physiology*, **33**, 264–271.

Rüger S., Netzer Y., Westhoff M., Zimmermann D., Reuss R., Ovadya S., Gessner P., Zimmermann G., Schwartz A., Zimmermann U. (2010a) Remote monitoring of leaf turgor pressure of grapevines subjected to different irrigation treatments using the leaf patch clamp pressure probe. *Australian Journal of Grape and Wine Research*, **16**, 405–412.

Rüger S., Ehrenberger W., Arend M., Geßner P., Zimmermann G., Zimmermann D., Bentrup F.W., Nadler A., Raveh E., Sukhorukov V.L., Zimmermann U. (2010b) Comparative monitoring of temporal and spatial changes in tree water status using the non-invasive leaf patch clamp pressure probe and the pressure bomb. *Agricultural Water Management*, **98**, 232–290.

Scholander P.F., Hammel H.T., Bradstreet E.D., Hemmingsen E.A. (1965) Sap pressure in vascular plants. *Science*, **148**, 339–346.

Smith D.M., Allen S.J. (1996) Measurement of sap flow in plant stems. *Journal of Experimental Botany*, **47**, 1833–1844.

Tyerman S.D., Tilbrook J., Pard C., Kotula L., Sullivan W., Steudle E. (2004) Direct measurement of hydraulic properties in developing berries of *Vitis vinifera* L. cv. Shiraz and Chardonnay. *Australian Journal of Grape and Wine Research*, **10**, 170–181.

Westhoff M., Reuss R., Zimmermann D., Netzer Y., Gessner A., Geßner P., Zimmermann G., Wegner L.H., Bamberg E., Schwartz A., Zimmermann U. (2009) A non-invasive probe for online monitoring of turgor pressure changes under field conditions. *Plant Biology*, **11**, 701–712.

Zimmermann U., Schneider H., Wegner L.H., Haase A. (2004) Water ascent in tall trees: does evolution of land plants rely on a highly metastable state? *New Phytologist (Tansley Review)*, **162**, 575–615.

Zimmermann D., Reuss R., Westhoff M., Geßner P., Bauer W., Bamberg E., Bentrup F.-W., Zimmermann U. (2008) A novel, non-invasive, online-monitoring, versatile and easy plant-based probe for measuring leaf water status. *Journal of Experimental Botany*, **59**, 3157–3167.

Zimmermann U., Rüger S., Shapira O., Westhoff M., Wegner L.H., Reuss R., Geßner P., Zimmermann G., Israeli Y., Zhou A., Schwartz A., Bamberg E., Zimmermann D. (2009) Effects of environmental parameters and irrigation on the turgor pressure of banana plants measured using the non-invasive, online monitoring leaf patch clamp pressure probe. *Plant Biology*, **12**, 424–436.

Zweifel R., Item H., Häsler R. (2000) Stem radius changes and their relation to stored water in stems of young Norway spruce trees. *Trees*, **15**, 50–57.

Zweifel R., Item H., Häsler R. (2001) Link between diurnal stem radius changes and tree water relations. *Tree Physiology*, **21**, 869–877.